*Physicochem. Probl. Miner. Process., 59(6), 2023, 175181* | Physicochemical Problems of Mineral Processing

http://www.journalssystem.com/ppmp | ISSN 1643-1049


# Evaluation of a capacity increase in AG milling of copper slag

**N. Metin Can [1], Orberk Mercan [2]**

[1] Hacettepe University, Department of Mining Engineering, Beytepe, Ankara, Turkey
[2] Al Masane Al Kobra Mining Co., P.O. Box 46 Najran, Saudi Arabia

Corresponding author: metin.can@hacettepe.edu.tr (N. Metin Can)

**Abstract:** The verification of the desired capacity increase in the grinding circuits is performed by simulation studies as they suggest accurate and fast alternatives compared to expensive and labor-intensive methods, particularly for the evaluation of situations that require investment. In this study, simulation was used to evaluate the alternatives that can be made to increase the capacity from 38.86 tph to 90 tph in a grinding circuit where copper slag is autogenously milled. The slag sample was characterized by drop weight and abrasion tests to describe the breakage in autogenous (AG) milling. The performances of the existing circuit and equipment were determined by a comprehensive sampling study, and modeling studies were carried out to form the basis of the simulations. Simulation scenarios were evaluated as investment free and investment requiring alternatives. In the investment free option changing fresh feed size distribution was examined however, capacity could be increased up to only 42 tph. In investment option, increasing the mill motor capacities was simulated and 90 tph target throughput was provided. This result was validated in the plant by replacement of mill motors of AG and pebble mill for 1000 kW and 750 kW, respectively.

*Keywords:* autogenous mill, copper slag, modelling, simulation, capacity

## 1. Introduction

Energy consumption at grinding stage is the biggest item among the energy costs of all mineral processes. Grinding costs are increasing, particularly with the depletion of deposits having coarse grain size of minerals and consequently the establishment of high-capacity plants. A great deal of effort has been made now by the mineral processing industry to understand an energy-intensive process such as grinding with mathematical models. As a result of the development of models with high predictive capacity, optimization studies in grinding circuits have been replaced by numerical evaluations rather than heuristic approaches. The model development for the process optimization of a given comminution circuit can be done in two ways. A common approach is to use the model structures of the machines to simulate the circuit where different process conditions and machine-related parameters are adjusted for the same final product specifications. The other approach is the integration of an optimizer to an existing model structure to estimate the optimal design and operating conditions (Muanpaopong et al. 2022; Muanpaopong et al. 2023). This study considered the common method of modelling where the existing model structures of the machines were utilized to simulate the circuit.

There are many approaches for mathematical modelling of autogenous mills (Stanley, 1974; Gault, 1975; Austin et al., 1976; Digre, 1979; Duckworth and Lynch, 1982; Barahona, 1984; Leung, 1987; Morrell, 2004). The kinetic approach was used in the model developed by Austin et al. (1976) in which the average residence time of the particles in the mill is used. For many years, JKMRC (Julius Krutschnitt Mineral Research Centre) has worked on the development of mathematical models of AG and semi-autogenous (SAG) mills based on data from a large number of pilot and industrial scale plants. The AG mill model depends on size mass balance approach (population balance model) of Epstein (1947). Whiten (1976) then developed the variation of it as given in Eq. 1. According to Whiten (1976), the size reduction processes that take place in the mill are shown as the breakage rate (ri) and the transport rate (di) for the material in each fraction. The breakage distribution function (aij) expresses the breaking

DOI: 10.37190/ppmp/175181

event; in other words, it determines how the j size of material will be distributed along the i size after the fracture. The mass balance for each particle size in the mill is written as follows:

$$f_i + \sum_{j=1}^{i} \left[\frac{a_{ij} * r_j * p_j}{d_j}\right] = p_i + \frac{r_i * p_i}{d_i} \tag{1}$$

where $f_i$ - mass flow of size fraction i in the feed, $a_{ij}$ - ppearance function (is the fraction of size j material broken into size i, $r_i$ - breakage rate of size fraction i, $p_i$ - mass flow of size fraction i in the product, $d_i$ - discharge rate of size fraction i.

In this equation rate of breakage, discharge function and appearance function parameters are of importance. For AG mill modelling, the given population balance equation was elaborated by many of the researchers with the aim of improving the predicting capability by considering these three functions. One of the major improvements was on the transport function where the discharge rate function was modelled by considering the particle size and process parameters such as pebble port, geometrical design of the mill etc. as reported by Morrell (2004) and Leung (1987). Latchireddi (2002) studied on better explanation of the grate design and pulp lifter parameters and the results were the following equations:

$$J_s = \eta \gamma^{n_1} A^{n_2} J_t^{n_3} \phi^{n_4} Q^{n_5} D^{n_6} \tag{2}$$

$$d_m = \frac{Q}{J_s} \tag{3}$$

where $J_s$ - the net fractional slurry hold-up inside the mill, $A$ - fractional open area, $J_t$ - fractional grinding media volume, $\phi$ - fraction of critical speed, $Q$ - slurry discharge flowrate, $\gamma$ - mean relative radial position of the grate holes, $\eta$ - coefficient of resistance which varied depending on whether flow was via the grinding media interstices or the slurry pool (where present), $n_{1-6}$ - model parameters, D - mill diameter, $d_m$ - constant rate.

Details of the calculation procedure of the appearance function are to be explained in the following section.

The power model developed by Morrell was also adapted to the Leung model (Morrell, 2004). For a better understanding of fracture, the combined fracture distribution function, which describes the material-specific impact and abrasion characteristics, has also been developed (Fig. 1).

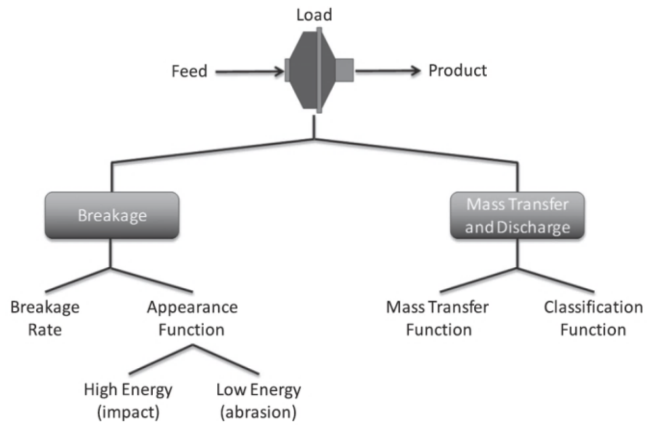


Fig. 1. Autogenous/semi-autogenous mill model after Leung (1987)

The perfect mixing model developed for ball mills is used in the modeling of the pebble mill in the grinding circuit in this study. The perfect mixing model, which is a combination of the kinetic and the matrix model, refers to the mill as a single unit that provides the perfect mix. In the model, it is admitted that the breaking event for each fraction entering and leaving a mill operating under continuous feeding condition is in equilibrium.

In the scope of classifier modelling, the approaches of Nageswararao (1995) and efficiency curve (Altun, 2007) were utilized for cyclone and screen units. Nageswararao model (1995) was stated as one of the accurate ones to predict the machine performance at varied geometries and operating conditions. It incorporates pulp hindered settling and viscosity factors. The model consists of three expressions predicting cut size, water split to underflow and throughput, are given by:

- Cut Size

$$\frac{d_{50c}}{D_c} = K_{do}(D_c^{-0.65})\left(\frac{D_o}{D_c}\right)^{0.52}\left(\frac{D_u}{D_c}\right)^{-0.47}\left(\frac{D_i}{D_c}\right)^{-0.50}\left(\frac{L_c}{D_c}\right)^{0.20}\theta^{0.15}\left(\frac{P}{\rho_p\, gD_c}\right)^{-0.22}\lambda^{0.93} \tag{4}$$

- Water Split

$$R_f = K_w(\lambda)^{0.27}\left(\frac{P}{\rho g}\right)^{-0.53}\left(\frac{D_o}{D_c}\right)^{-1.19}\left(\frac{D_u}{D_c}\right)^{2.40}\left(\frac{D_i}{D_c}\right)^{-0.50}\left(\frac{L_c}{D_c}\right)^{0.22}\theta^{-0.24} \tag{5}$$

$$R_v = K_{v1}\left(\frac{P}{\rho_p gD_c}\right)^{-0.53}\left(\frac{D_o}{D_c}\right)^{-0.94}\left(\frac{D_u}{D_c}\right)^{1.83}\left(\frac{D_i}{D_c}\right)^{-0.25}\left(\frac{L_c}{D_c}\right)^{0.22}\theta^{-0.24} \tag{6}$$

- Throughput

$$Q = K_{q1}{D_c}^2\left(\frac{P}{\rho_p}\right)^{0.50}\left(\frac{D_o}{D_c}\right)^{0.68}\left(\frac{D_i}{D_c}\right)^{0.45}\theta^{-0.10}\left(\frac{L_c}{D_c}\right)^{0.20} \tag{7}$$

where $K_{q1} = K_{q0}{D_c}^{-0.10}$, $d_{50c}$ - corrected cut-size (μm), $D_c$ - cyclone cylinder diameter (m), $K_{do}$ - depends on feed solids characteristics only (size distribution and specific gravity), $D_o$ - overflow (vortex finder) diameter (m), $D_u$ - underflow (apex) diameter (m), $D_i$ - inlet diameter (diameter of circle of same area as cyclone inlet) (m), $L_c$ - Length of cylindrical section (m), p - feed pressure at inlet (kPa), $\rho_p$ - feed slurry density (t/m$^3$), g - acceleration due to gravity (9.81 m/s$^2$), λ - hindered settling correction term=$10^{1.82C}$v/(8.05[1-Cv)$^2$), θ - cone full angle (degrees), $R_f$ - recovery of water to underflow (%), $K_{q0}$ D-depends on feed solids characteristics (eg. specific gravity) only, $K_{q1}$ - the proportionality constant (function of the feed material and diameter of the cyclone), $K_w$ - constant in the water recovery relationship, Q - flowrate (m$^3$/h).

Single component efficiency curve predicts the Tromp Curve (Napier-Munn et al., 1996) of the classifier and the stream properties, i.e., solids content and size distributions, with the least margin of error as stated by many of the researchers (Whiten,1976;Altun, 2007). The model expression is given by:

$$E_0 = \frac{C(1+\beta\beta'\frac{d}{d_{50c}})(e^{(\alpha)-1)})}{(e^{\left(\alpha*\beta'\frac{d}{d_{50c}}\right)}+e^{(\propto)-2)}} \tag{8}$$

where $E_0$ - fraction of feed reporting to overflow, d – size, $d_{50c}$ - size of a particle in feed which has equal probability of reporting to underflow or overflow, C - the fraction undergoing "real" classification, α - sharpness parameter of the curve, β - fishhook parameter of the curve, β′ - a parameter to preserve the definition $d_{50c}$.

Autogenous milling may include different circuit designs depending on the mineral types and concentrations in the ore and its downstream treatment. Generally, autogenous milling applications are operated as open circuits, but circuit designs in which coarse particles are classified by trommel sieve or vibrating sieve and recirculated to the mill are also encountered (Gupta and Yan, 2016). In some cases, instead of recirculating coarse fraction, the oversize material is sometimes prevented from discharging by using a reverse spiral at the end of the mill and washes back into the mill (Napier-Munn et al., 1996). In addition to open circuit applications, autogenous mills can also be operated in closed circuit with a fine classifier or a crusher. When they are operated in closed circuit with hydrocyclones, the throughput capacity is lower than the open circuit application due to the excess material recirculating from the hydrocyclone underflow. The configuration in which the mill is operated in a closed circuit with the crusher has been widely preferred in recent years, as it is very effective in increasing the raw feed capacity. As critical size material (25-50 mm), which builds up in the mill, removed in this configuration, mill load is reduced, thus capacity increase can be accomplished. There are also circuits where the hydrocyclone and pebble crusher are operated together with the autogenous mill. As the coarse particles in the mill are broken in the crusher, the preferred grinding media for the fine particles cannot be provided, so quite coarse flow is taken from the hydrocyclone overflow. Thus, this may lead to a reduction in feed capacity to obtain the required fineness of hydrocyclone product (Napier-Munn et al., 1996). Use of HPGR in the circuit design has also been considered particularly for hard ore processing. Selection of appropriate circuit configuration is strongly influenced by plant capacity and ore competence (Foggiatto, 2017).

This study tested the hypothesis of showing the path for the improved energy efficiency or production rate of the given comminution circuits by using a simulation software. The novelties of the study can be explained in many ways. The literature on copper slag grinding circuits and their optimization is scarce. However, its importance is well-known since tailing management and the metal recoveries from the tailings are the major concerns of the mineral processing and metallurgy. Moreover, the simulation without the plant validations has a risk of questioning its applicability. In this study the simulations were performed, and its outcomes were validated by the plant. In brief, the study aimed at increasing the existing production rate of the copper slag grinding circuit to 90 tph by considering investment (such as mill motor replacement) and non-investment (changing feed size distribution) alternatives. It is believed that the experience and the outcomes of the research can be useful both for academia and industry.

## 2. Materials and methods

### 2.1. Sampling

The ore used in the tests was taken from a copper slag grinding circuit existing in a smelter plant. The studies were carried out in two stages as plant sampling and laboratory studies. The grinding circuit consists of autogenous (5.65mx4.20m) and pebble mills (3.35mx2.50m), double-deck sieve and hydrocyclone groups. The current values drawn by the AG and pebble mills were monitored during the sampling study (Fig. 2) and sampling was performed at the steady-state operating condition of the circuit. The sampling points are illustrated in Fig. 3. According to the data recorded from control room, the solid flowrate of the feed to autogenous mill was 38.86 tph, the Cu grades of 1st hydrocyclone overflow and Cu concentrate were 4.02% and 35.71%, respectively.

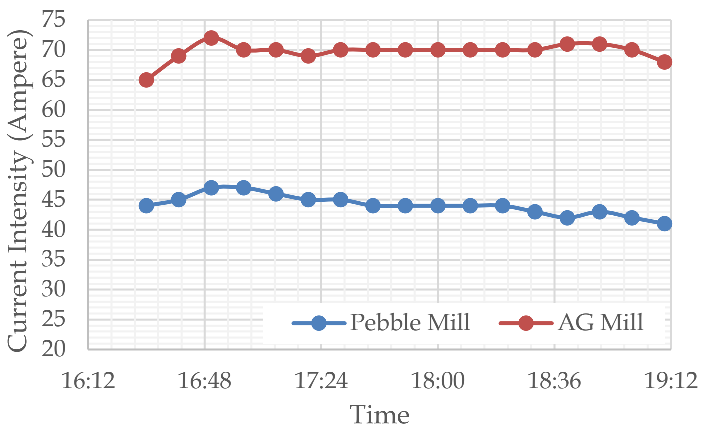


Fig. 2. Variation of current intensities drawn by the mills with time

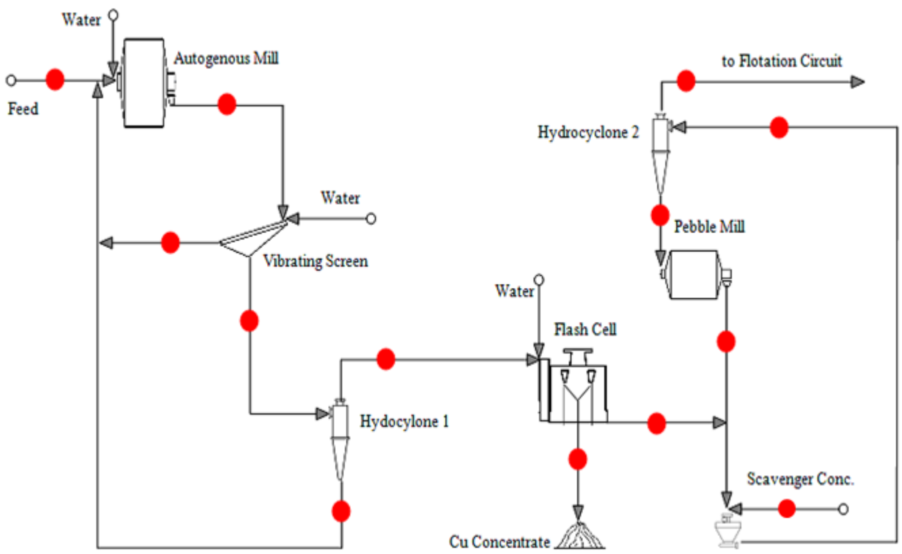


Fig. 3. Sampling points around the grinding circuit

The detailed drawings of the mills required for both mathematical modeling studies and the calculation of the grid open area, the power measurements during the sampling period and the measurements of the hydrocyclones were provided. The volumetric total loads of both mills were noted as 18%, while the rotation critical speeds were recorded as 70% and 75% for AG and pebble mill, respectively. Pebble size in the pebble mill was 50 mm. The particle size distribution, solid contents and volumetric flow values of the streams were determined by analyzing the samples taken around the autogenous grinding circuit. The data obtained from the 1st sampling period was used for mass balance and modelling studies.

### 2.2. Characterization of ore

Particle size distributions of all samples were measured by wet sieving down to 38μm size. Laser diffraction method was preferred for the samples around hydrocyclones as it was possible to determine the lower limit of the size down to 1.8μm.

The grindability parameters of the slag were determined for use in modelling and simulation studies. Bond Work Index was measured as 19 kWh/t for 106μm test sieve.

Since the breakage of the particles in autogenous grinding occurs in two main modes as high and low energy, drop weight and abrasion tests were conducted respectively to characterize the fracture of the slag at these energy levels (Napier-Munn et al., 1996; Lynch, 1977). For explaining the appearance function, the combination of "tn" (high energy appearance function) and "ta" (low energy appearance function) were used (Napier-Munn et al., 1996). The drop weight test results were used to express the "tn" function. In this regard, $t_{10}$ index, which is defined as the percent of breakage product that passes 1/10 of the initial size, is calculated by using the Equation given below. This index is related to the specific energy input as follows:

$$t_{10} = A * (1 - e(-Ecs*b)) \tag{9}$$

A and b ore-specific parameters were determined by nonlinear regression technique (Narayanan and Whiten, 1988). Parameter A shows the maximum value of $t_{10}$. It states that no more fine material can be formed after a certain energy level. A*b value represents the slope of the curve when the specific energy of comminution is zero. The ore-specific A and b parameters obtained as a result of the drop weight test are used in mill modelling for predicting how ore breaks inside the mill. Drop-weight test was carried out according to the standards defined by JKMRC to determine how the material will break due to impact. The energy levels and particle size ranges conducted at the test are given in Table 1.

Table 1. The energy levels and particle size ranges for drop-weight test

| Energy Levels | -63+53mm | -45+37.5mm | -31.5+26.5mm | -22.4+19.0mm | -16+13.2mm |
|---|---|---|---|---|---|
| 1st (kWh/t) | 0.05 | 0.10 | 0.25 | 0.25 | 0.25 |
| 2nd (kWh/t) | 0.08 | 0.25 | 1.00 | 1.00 | 1.00 |
| 3rd (kWh/t) | 0.10 | 0.40 | 1.30 | 2.50 | 2.50 |

The value of parameter A was 58.37, parameter b was calculated as 1.33 t/kWh. The graph showing the $t_{10}$ fineness index values versus the specific comminution energy (Ecs) values is given in Fig. 4a. The breakage function used in the study considered normalized form and its plot is also illustrated in Fig. 4b.

"Ta" (low energy) is the parameter to define the abrasion property of the ore and is performed within a 300*300 mm drum mill used within the standards determined by JKMRC (Napier-Munn et al., 1996). A 3 kg test sample with a particle size range of -55+38mm was milled for 10 minutes at a speed of about 53 rpm, which corresponds to 70% of the critical speed. The abrasion breakage value of the sample is expressed with "$t_a$" parameter, and it corresponds to 1/10 of the $t_{10}$ value determined from the sieve analysis. A high value of "$t_a$" means that the ore has a low resistance to abrasion breakage. Accordingly, the ground sample was sieved dry and the amount of material passing the $t_{10}$ value was calculated as 3.70% and the "ta" parameter as 0.37.

In the final state of the appearance function equation, high and low energy "t" values together with the appearance functions are inputted to obtain a combined appearance function (Eq. 1). The formula is roughly the weight average considering the ratio to total “t” values as given by Napier-Munn et al. (1996).

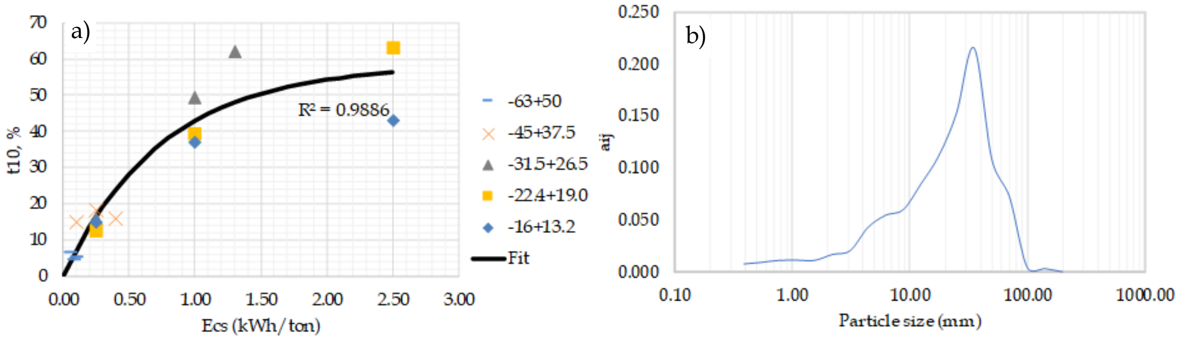


Fig. 4. a) Relationship between the specific comminution energy (Ecs) and $t_{10}$ b)aij as a function of particle size

### 2.3. Mass balance, modelling and simulation

After sampling, the values of solid contents and the particle size distributions of all streams were used in mass balance study which was carried out using JKSimMet v6.01 software. Solid and volumetric flowrates, percentage of solid contents and the particle size distributions of each stream were balanced. Predicting successful and most realistic scenarios with simulation is based on the establishment of reliable models of all equipment in the circuit after correct mass balance studies. The model developed by Leung (1987) was used in the mathematical modeling of the autogenous mill. In the pebble mill, mathematical modeling was done by using the perfect mixing module. Single component efficiency curve was used for modelling of hydrocyclone and sieve. Model parameters were calculated with JKSimMet v6.01 by evaluating the particle size distribution and tonnage at the streams around each equipment. Followed by modelling the grinding circuit with the balanced data of sampling period, the base simulation condition was obtained. The base simulation condition is accepted as the benchmarking of all simulation studies for capacity increase. In all simulation studies, data were produced as a result of changing a single variable by keeping all variables constant thus, it enabled the comparison of the effects of the results with the base simulation condition.

## 3. Results and discussion

### 3.1. Mass balance

It is seen that the reconciliation of all data measured and calculated were good indicating the quality of the sampling data was proper for equipment modelling (Fig. 5).

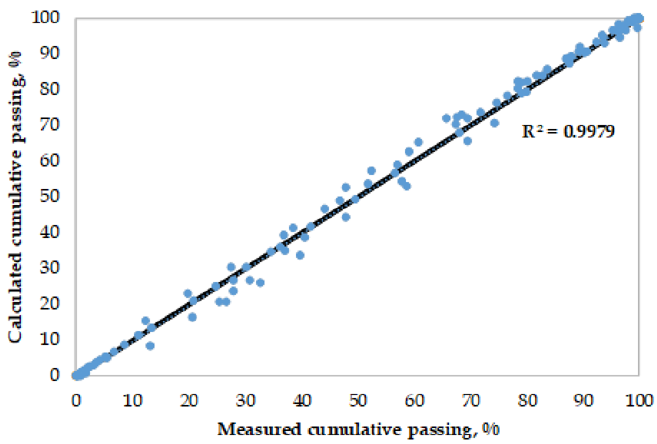


Fig. 5. Reconciliation of measured and calculated particle size distributions for all streams

Mass balance of the circuit including solids flowrates (tph), solids %, $p_{80}$ (mm) and volumetric flows ($m^3$/h) are shown in Fig. 6. The particle size passing 80% of the raw feed and autogenous mill feed were calculated as 120.87mm and 37.44mm, respectively. The capacity of the circuit was 38.86 tph and the reduction ratio of the autogenous mill was calculated as 23.02. It was determined that approximately 89% of the Flash unit cell concentrate was finer than 38µm.

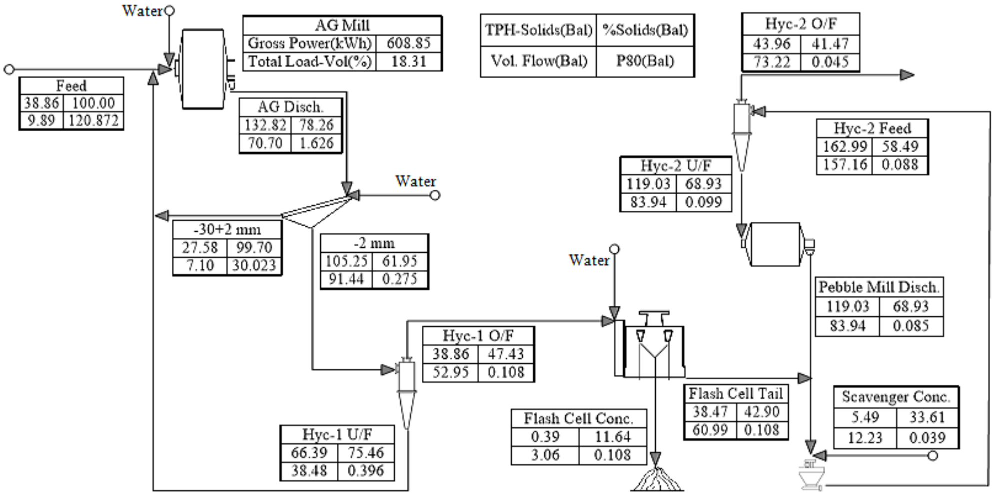


Fig. 6. Mass balance of the circuit for the first period of sampling

### 3.2. Modelling

In the autogenous mill model, it is seen that the balanced particle size distributions of the mill feed and product, and the data estimated by the mathematical model are in good agreement (Fig. 7a). The breakage rate function calculated according to Leung model is given in Fig. 7b. The shape of the breakage rate for the autogenous mill includes two regions of breakage and it is due to the nature of the grinding environment. Within an autogenous mill the first breakage occurs on the surface (in the toe region) due to the impact. The further breakage is caused by the rotation of mill where the charge does not move but the layers of particles slip over each other (abrasion and attrition). Abrasion breakage affects the coarser particles, and it can be stated that its rate reduces from the top size to a minimum, which is usually 25-50mm. These critical sized particles are crushed by the larger rocks (impact) and then leave the mill hence the breakage rate increases down to 2-5mm range where another peak is observed (Napier-Munn et al., 1996). This peak depends both on the broken particles coming from the coarser sizes and the increased discharge rate of these sized particles. As the water flow affects the particles, their probability of breakage reduces considerably as their rate of discharge increases. In the Leung model based on the mass transfer law, the mass transfer constants called m1 and m2 were taken as 0.37. These values were obtained as a result of pilot scale tests conducted by Leung. Optimum grid opening, which was one of the model parameters, was determined as 43.80mm. The particle size which has a fluidity behavior in the mill and defines the fine size, was determined as 0.042mm. As a result of the modelling, the power consumed by the autogenous mill was estimated as 679.89 kW/h. This value shows the power value transferred directly to the charge. Despite the information that the installed power of the mill is 750 kW/h, this value was measured as 722 kW/h during the sampling period. The mill load was calculated as 21.96% by the model.

The perfect mixing model was used for modelling of the pebble mill. Balanced and the modelled particle size data from feed and the discharge of the mill is illustrated in Fig. 8a. The breakage/discharge rate function can be calculated as in Fig. 8b for each particle size when the size distributions of the mill feed and discharge, and the breakage function are known. This curve is expressed with the cubic spline function and the function formed using the nodal points determines the pebble mill performance. In the breakage/discharge rate curve, it is seen that the breakage rate increased for particles up to 0.276mm size and these particles left the mill by acting more fluidly. In coarser sizes, it is understood that the breaking/discharge rate of the particles decreased, and they were subjected to classification within the mill.

The modeling of the sieve at the discharge of autogenous mill (Fig. 9a) and hydrocyclones were performed using single-component efficiency curve (Fig. 9b and 9c).

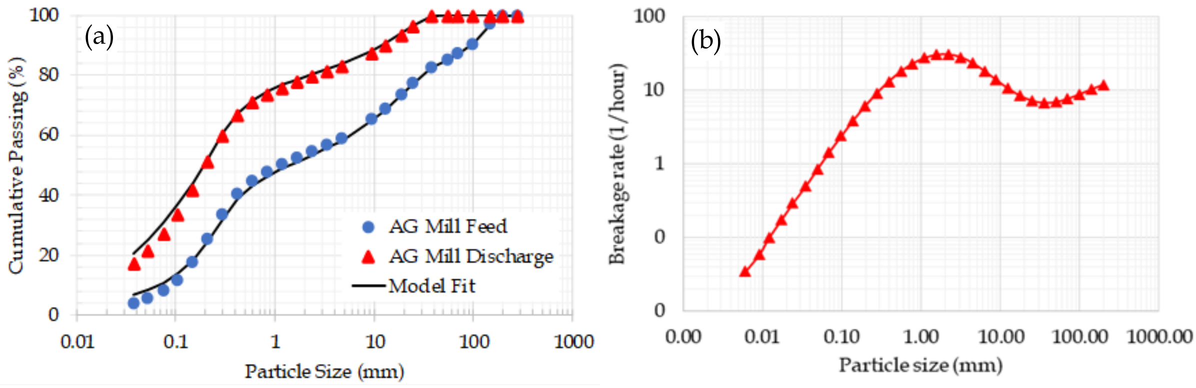


Fig. 7. (a) Model fit data for autogenous mill (b) Breakage rate function

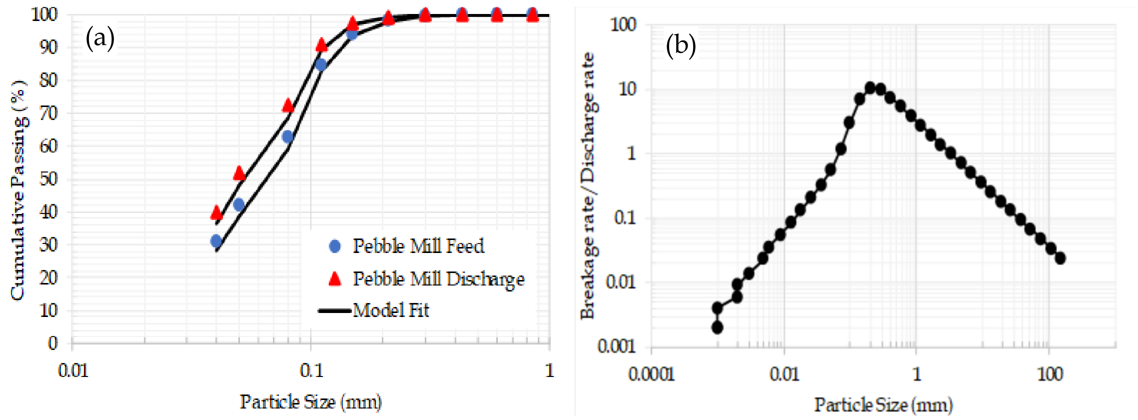


Fig. 8. (a) Model fit data for pebble mill (b)Breakage/discharge rate function

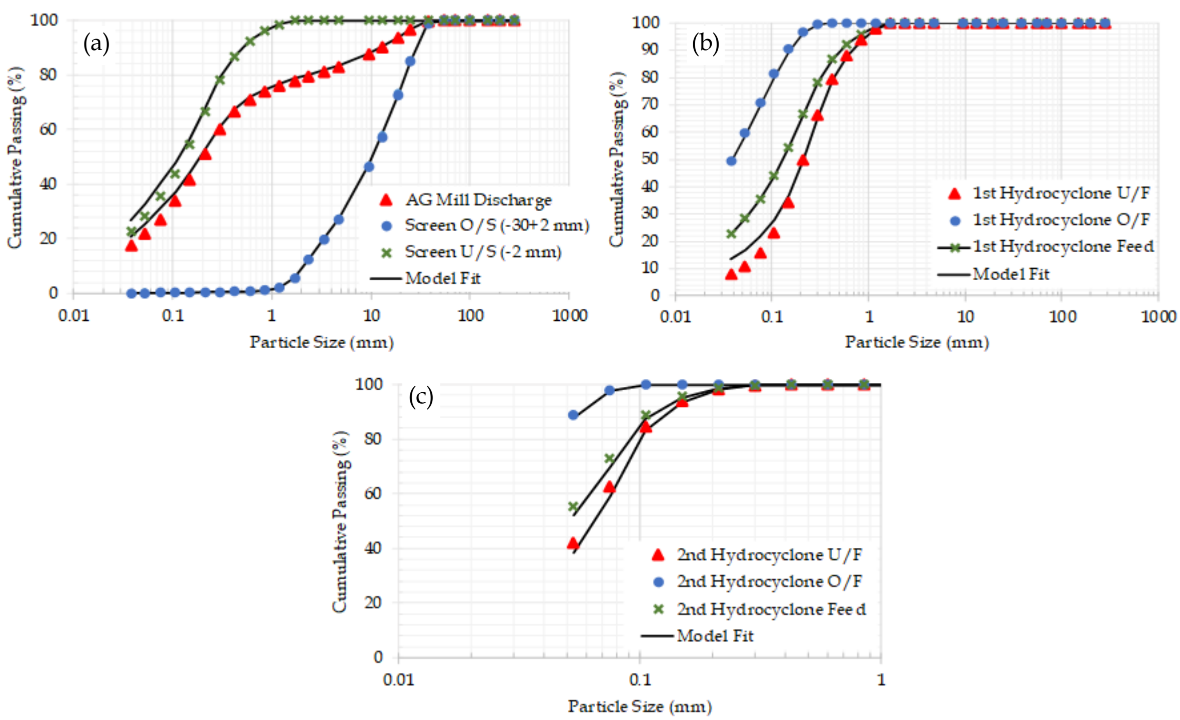


Fig. 9. Model fit data for (a) sieve (b)1st hydrocyclone group and (c)2nd hydrocyclone group

The values of the model parameters obtained according to the single-component efficiency curve for the classifier equipment are given in Table 2 and Table 3.

Table 2. Model parameters of the screen in the circuit

| Parameters | Single Deck Sieve |
|---|---|
| Slope of the curve, $\alpha$ | 7.446 |
| Fishhook, $\beta$ | 0.000 |
| By-pass, % | 99.868 |
| $d_{50c}$, mm | 1.473 |
| Corrected, $\beta^*$ | 1.000 |

Table 3. Model parameters of the hydrocyclones

| | Simulation (base condition) | |
|---|---|---|
| | Cyclone (AG mill) | Cyclone (Pebble Mill) |
| $K_{D0}$ | 6.34E-05 | 8.06E-05 |
| $K_{Q0}$ | 74.9 | 494.6 |
| $K_{V1}$ | 31.12 | 16.87 |
| $K_{W1}$ | 83.24 | 52.58 |
| Alpha | 1.96 | 3.49 |
| Beta | 0.01 | 0.01 |
| # of cyclones in operation | 3 | 3 |
| operating pressure (kPa) | 95 | 101 |

### 3.3. Simulation studies for improved throughput

The study aimed at finding a solution to improve the throughput of the circuit to 90 tph by considering the scenarios with investment (additional machines or replacement of the existing ones) and no-investment (change in the process conditions) cases. Table 4 summarizes the alternatives tested throughout the evaluations.

Table 4. Summary of the simulations

| | Investment | No-investment |
|---|---|---|
| Sim #1 | | Change in the feed size distribution |
| Sim #2 | Increasing the mill motor capacities (validated) | |

Prior to proceeding with the detailed evaluations, it is of importance to depict the output of base case simulation and its agreement with the mass balanced data. Fig. 10 illustrates the simulated flow rates of the streams as well as the power draws of the AG and pebble mills. The calculations agreed with the mass balanced size distributions and the solids content, which are depicted and summarized in Fig. 11 and Table 5.

The simulation studies implied that the data can be utilized in further stages where different alternatives to be considered to reach 90 tph production rate.

Table 5. Comparison of mass balance and base simulation condition

| Streams | Mass balance condition | | | Base simulation condition | | |
|---|---|---|---|---|---|---|
| | Solid, tph | Solid, % | $P_{80}$, mm | Solid, tph | Solid, % | $P_{80}$, mm |
| Autogenous Mill Discharge | 132.82 | 78.26 | 1.63 | 131.49 | 78.26 | 2.26 |
| 1st Cyclone U/F | 66.39 | 75.46 | 0.40 | 62.93 | 78.40 | 0.44 |
| 1st Cyclone O/F | 38.86 | 41.43 | 0.11 | 38.86 | 46.23 | 0.11 |
| 2nd Cyclone Feed | 162.98 | 58.49 | 0.09 | 161.15 | 55.97 | 0.09 |
| 2nd Cyclone U/F | 119.03 | 68.93 | 0.10 | 117.19 | 66.81 | 0.10 |
| 2nd Cyclone O/F | 43.96 | 41.47 | 0.045 | 43.95 | 39.07 | 0.04 |
| Pebble Mill Discharge | 119.03 | 68.93 | 0.085 | 117.19 | 66.81 | 0.09 |

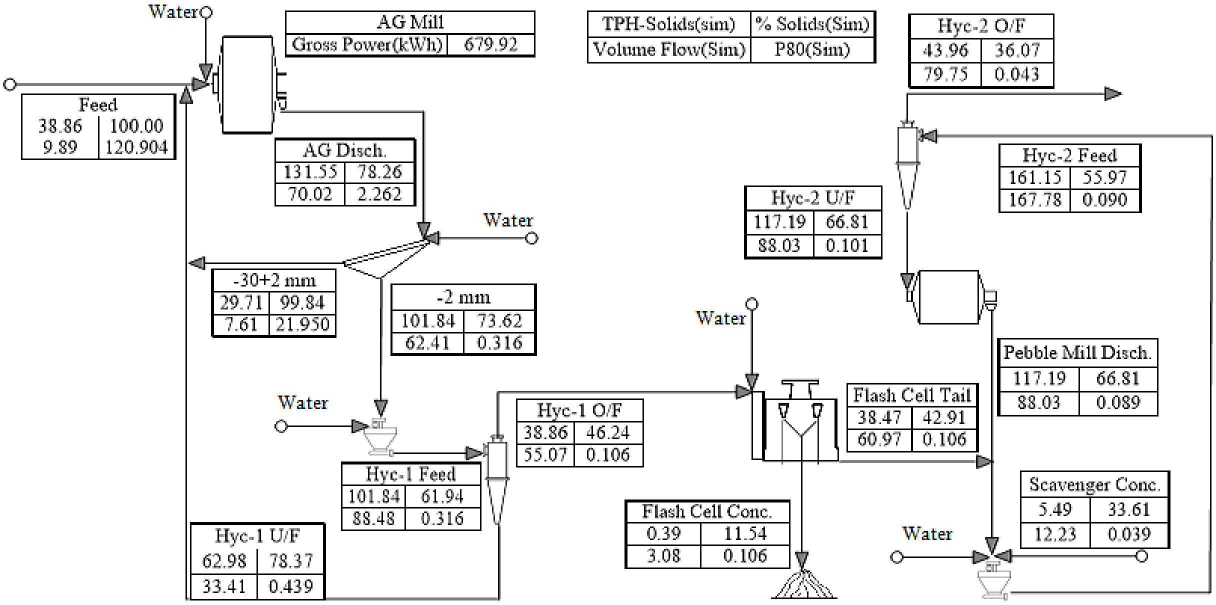


Fig. 10. Simulation output of the base case

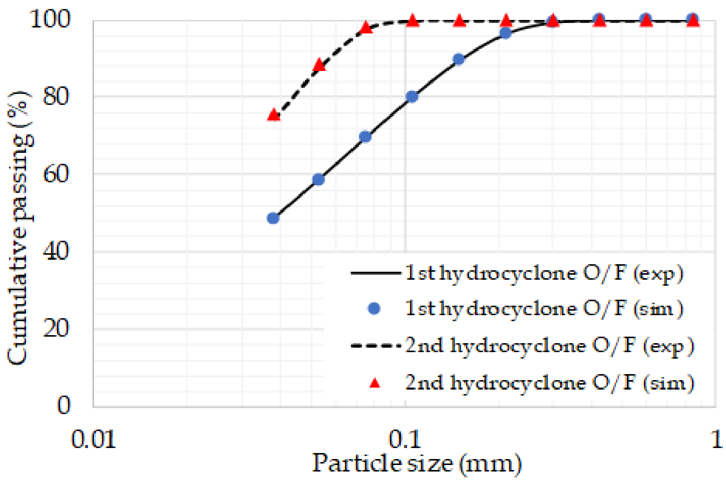


Fig. 11. Experimental and simulated cyclone overflow size distributions

### 3.3.1. Changing the feed size distribution (Sim #1)

It is a well-known fact that feed ore properties such as hardness and particle size distribution have a great impact on the performance of autogenous milling. The parameter that will most easily affect the increase in the capacity of the grinding circuit and maintaining the target particle size of the ground product is to change the particle size distribution of the raw feed (Hahne et al., 2003; Bueno et al., 2013). The particle size distributions tested in the simulation studies are given in Fig. 12. The 1$^{st}$ particle size distribution was the size distribution of the plant feed at the current sampling condition. The 2$^{nd}$ particle size distribution was obtained in the Gaudin and Schuhmann equation, when the α parameter was taken as 0.5. The 3$^{rd}$ particle size distribution represented the distribution obtained from the plant in previous studies. The 4$^{th}$ particle size distribution was obtained by sieving the raw feed through a 100mm sieve and mixing the overflow and underflow material of the sieve at the rates of 65% and 35%, respectively. It was determined that no particles coarser than 200mm in size were found in the mill feed during sampling. Therefore, the effect of such a mixture was investigated considering that the presence of coarse particles in the feed would provide a better grinding media in the autogenous mill. In the simulation studies with these size distributions, it was possible to increase the raw feed tonnage from 38.86 tph to 42 tph.

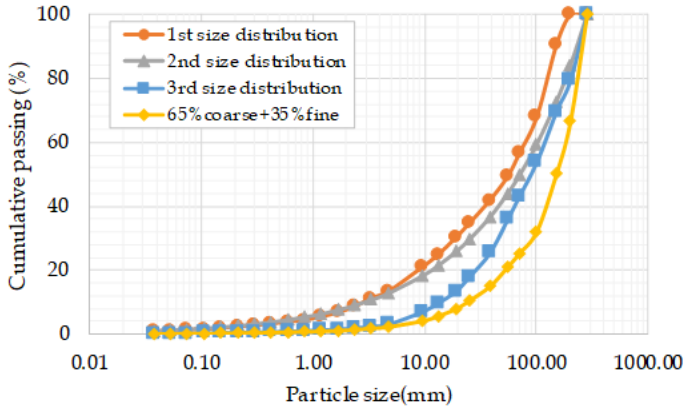


Fig. 12. Different particle size distributions used in simulation studies

Flowrates and $p_{80}$ values obtained as a result of the simulation study using the 2nd particle size distribution data are shown in Fig. 13. With this distribution, it is seen that the power consumption of the autogenous mill decreased from 679.89 kWh (the base simulation condition value) to 590.40 kWh. In addition, by increasing the particle size of the autogenous mill product, the return load to the mill was reduced. Similar findings have been reported by other researchers (Morrell and Valery, 2001; Behnamfard et al., 2020) in the literature, which has been noted that the mill weight and power draw decrease as the top size of the feed ore increases.

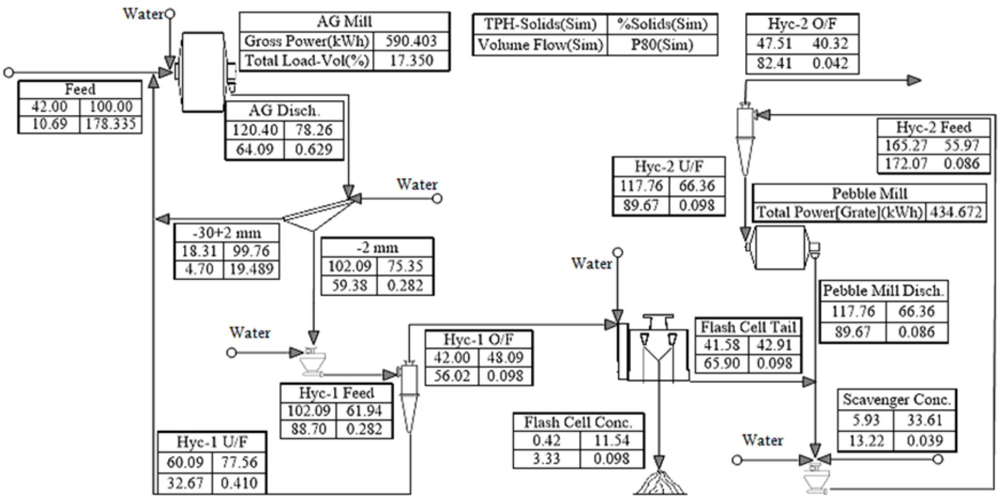


Fig. 13. Best simulation scenario with changing of particle size distribution of feed

In the 3rd and 4th particle size distribution alternatives, the power values of the autogenous mill were calculated as 609.86 kWh and 646.05 kWh, respectively. Although it was lower than the base condition, it was found to be higher than the 2nd distribution alternative. However, it was not possible to increase the grinding circuit capacity to 90 tph in any of the alternatives for changing the feed particle size.

### 3.3.2. Increasing the Mill Motor Capacities (Sim #2)

The previous assessment proved that changing the feed size distribution alternative was not able to produce 90 tph. Therefore, further evaluations focused on increasing the mill motor power that meet the need for the increased throughput. Improving the processing capacity of a mill is primarily design dependent. Besides the effective diameter and length, it might be possible to replace the main motor with an increased one hence the mill can rotate the higher loads effectively. As this study aimed at achieving higher throughputs, the focus was given on the motor replacement of which the quantity was calculated by using the power models in the literature. Gao et al. (2020) also followed a similar approach in their mill optimization study and the relationship between the mill motor power and the processing capacity was depicted. In this context, several calculation steps were undertaken by benefiting from the current models (Napier-Munn et al., 1996) and approaches (Bond, 1952) which enables selecting the required power draw for a given feed and product size together with the throughput. These calculations were undertaken in 2 steps. Initially, AG mill power draw was predicted and secondly, the product of AG-Hydrocyclone circuit was considered to reduce the size down to $d_{80}$ of 45µm, which was the target. Table 6 tabulates the existing installed and operational power draws of the mills.

Table 6. Installed power draws of the mills

| | Actual installed power (kW/h) | Operational power (kW/h) |
|---|---|---|
| AG mill | 750 | 722 |
| Pebble Mill | 530 | 425 |

To find out the required power draw of AG mill, the model developed by Napier Munn et al. (1996) was used. The overall model structure is given below:

$$\text{Gross power} = \text{No-load power} + (k \times \text{charge motion power}) \tag{10}$$

where Gross power - power input to the motor, i.e., metered power, No-load power - power input to the motor when mill is empty, k × charge motion power - net power, Net power - total power input to the charge, k - lumped parameter which accounts for heat losses due to internal friction, energy for attrition/abrasion/breakage and rotation of the grinding media, plus inaccuracies associated with assumptions and measurement of the charge shape and motion

Fig. 14 illustrates the simulation output once the feed rate was changed for the same ore characteristics.

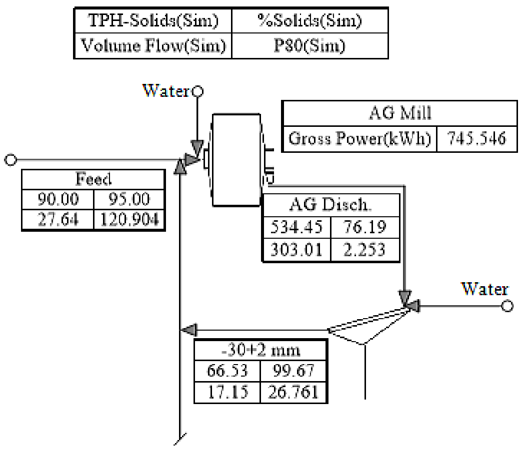


Fig. 14. Simulation results at increased feed rate

As seen in Fig. 14 the AG power draw of 745 kW is required to process 90 tph of feed.

For the pebble milling, the approach developed by Bond was considered to calculate the required power draw to reduce the $d_{80}$ of 100µm to 45µm. When the efficiency factors such as optimal feed size, required product size, mill diameter as well as the work index of the ore are considered (19 kWh/t), the required power draw of the mill was found to be 698 kW.

The results concluded that the power draw of the mill should be improved to at least 1000 kW and 800 kW for AG and pebble milling, respectively. The complete simulation of the circuit at 90 tph is depicted in Fig. 15.

### 3.3.3. Plant validation of the motor replacement option

Since the study would be incomplete without validation, this section aimed at sharing the outcomes of the applied modification at the plant directly that the option of motor replacement was of interest for the capacity improvement. The action that the plant chose was to purchase a 1000 kW motor size for the AG mill and install its 750 kW motor to pebble mill. The motor replacement option has been preferred for the following reasons as well as providing the capacity increase of the circuit:

- To protect the motor health of the AG mill for a long time,
- Providing a more sustainable operation and less shutdowns
- Solving the grinding bottleneck in the pebble mill

Such modification meets the demand of the required power input as calculated previously.

Once the plant completed all the installations, another survey was held at steady-state, samples were collected for four hours and then mass balancing calculations were performed (Fig. 16).

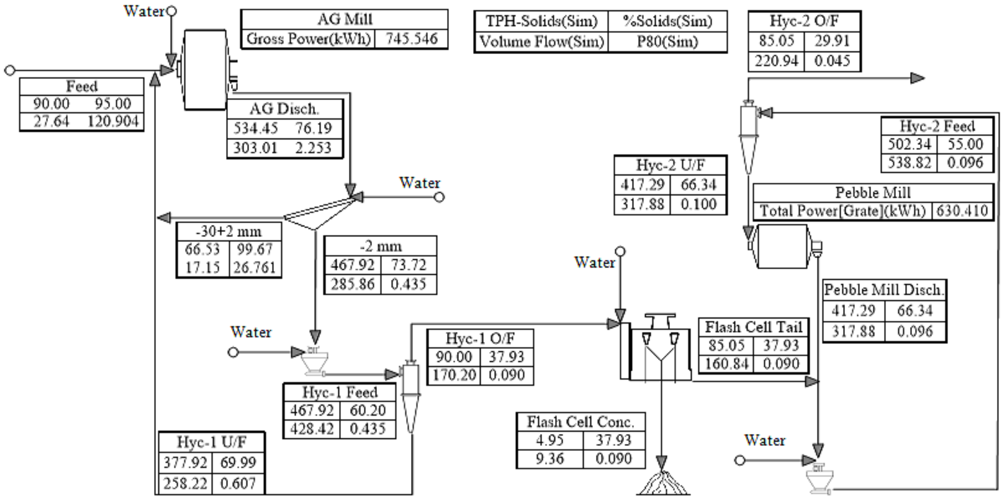


Fig. 15. Full circuit simulation at 90 tph

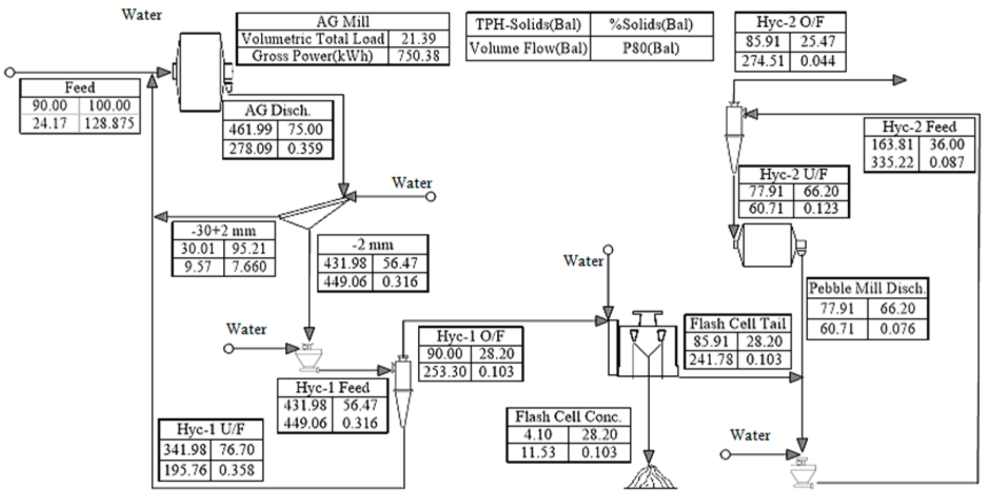


Fig. 16. The mass balanced condition of the plant after the modifications

Table 7 summarizes the comparison between the simulation results (Fig. 15) and the actual plant operation (Fig. 16). The impact of motor replacement is also illustrated as the comparison of particle size distributions of 1st and 2nd hydrocyclone overflow streams in Fig. 17. While particle size distribution of the 2nd hydrocyclone group are almost same as each other, a difference in size distribution of 1st group of hydrocyclones before and after the motor replacement is seen. Such variation can be attributed to the dynamics of AG milling circuit as its operation is highly influenced by the fluctuations in the feed ore characteristics. The same comment is valid for the differences in the solids content of overflow streams. Although a noticeable difference exists in the 1st cyclone overflow, the results of the 2nd cyclone are close to each other. Conducting a validation study aims at achieving the required throughput and the target size of the final product hence the operators give focus on these parameters. Mostly, the fluctuations in the middle processes, like 1st cyclone, may happen due to the milling fluctuations in AG and this may cause some variations in the predictions. However, as mentioned, the simulation had the best fit for the final product size and the throughput.

Table 7. Summary of the simulation and actual plant operation

| | Simulation results | | Plant results | |
|---|---|---|---|---|
| | Solid, tph | Solid, % | Solid, tph | Solid, % |
| Autogenous Mill Discharge | 534 | 76 | 462 | 75 |
| 1st Cyclone O/F | 90 | 38 | 90 | 28 |
| 2nd Cyclone O/F | 85 | 30 | 86 | 26 |
| Power draw of AG mill (kW) | 745 | | 750 | |
| Power draw of pebble mill (kW) | 698 | | 648 | |

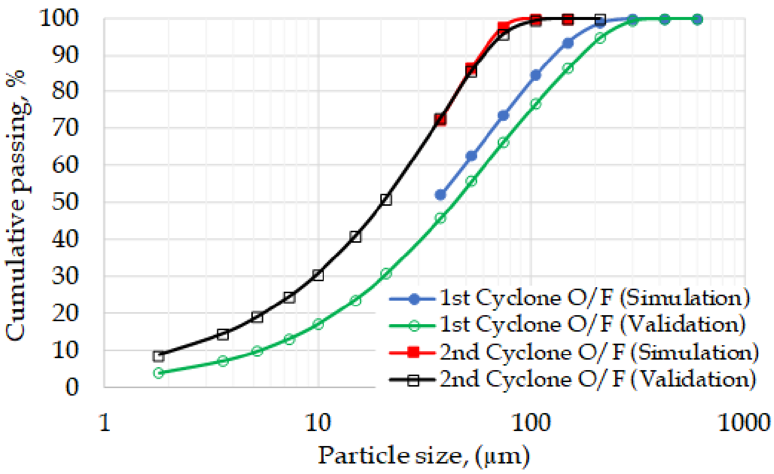


Fig. 17. Particle size distributions

## 4. Conclusions

This study discusses the evaluation of changes that can be made to the grinding circuit to increase capacity and performance in an existing smelter through modelling and simulation. Followed by modelling the grinding circuit with the balanced data of sampling period such as tonnage, solids % and $p_{80}$ values, the base simulation condition was obtained. As these values were in good agreement, it was decided that the base simulation condition could be the benchmark of all the simulation studies. Improvements to increase fresh feed capacity were evaluated under two groups of simulation scenarios as investment free and investment requiring alternatives.

Controlling the size distribution of the autogenous feed is one of the most important parameters in grinding performance therefore, within the scope of no-investment case, the effects of change in autogenous feed particle size were examined. Four different particle size distribution options were simulated. Among the conditions studied, it was determined based on the estimated power draw that the presence of particles coarser than 200mm in the feed could create a better grinding environment in the autogenous mill. Nevertheless, none of which option provided the required increase in feed capacity.

In the second simulation scenario the investment option was evaluated; the required motor powers of AG and pebble mills that will process 90 tph of throughput and produce the required $p_{80}$ size product were estimated. The simulation results showed that capacity increase was achieved, and the power draw of the mill should be improved to at least 1000 kW and 800 kW for AG and pebble milling, respectively. This outcome was confirmed by validation tests that covered the replacement of mills' motors at the plant. The plant management preferred to purchase a 1000 kW motor size for the AG mill and install its 750 kW motor to pebble mill considering solving some bottlenecks in operational parameters.

This study has demonstrated that simulation based on accurate models is an excellent tool in the decision-making process of possible improvement alternatives to improve the performance of circuits. As a result of this study, it was determined that the capacity of the grinding circuit could be increased to 710000 tons/year with 90% availability.

**Acknowledgments**

The authors would like to express their sincere thanks to Prof. Ş. Levent Ergün and Assoc. Prof. Okay Altun for their valuable contributions.

**References**

ALTUN, O. 2007. *Comparison of different efficiency curve approaches in modelling of air classifiers*. Dissertation, Hacettepe University, Turkey.

AUSTIN, L.G., WEYMONT, N.P., PRISBREY, K.A., HOOVER, M., 1976. *Preliminary results on the modelling of autogenous grinding*. In: 14th International APCOM Conference, The Pennsylvania State University, 207–226.

BARAHONA, C.A. 1984. *Modelling and simulation of semi-autogenous grinding systems*. Dissertation, The Pennsylvania State University.

BEHNAMFARD, A., ROUDI, D.N., VEGLIO, F. 2020. *The performance improvement of a full-scale autogenous mill by setting the feed ore properties*. J. Cln. Prod., 271, 122554 https://doi.org/10.1016/j.jclepro.2020.122554.

BOND, F.C. 1952. *The third theory of comminution*. Trans SME/AIME, 169, 58-66.

BUENO, M.P., KOJOVIC, T., POWELL, M.S., SHI, F. 2013. *Multi-component AG/SAG mill model*. Min. Eng., 43-44, 12-21.

DIGRE, M. 1979. *Autogenous grinding testing and scale up*. Proceedings of the Autogenous Grinding Seminar. Trondheim, Norway Paper F5.

DUCKWORTH, G.A., LYNCH, A.J. 1982. *The effect of some operating variables on autogenous grinding circuits and their implications for control*. XIV International Mineral Processing Congress. Toronto, 1.1-1.21.

EPSTEIN, B. 1947. *The material description of certain breakage mechanisms leading to the logarithmic-normal distribution*. J. Franklin Inst., 244–471.

FOGGIATTO, B. 2017. *Modelling and simulation approaches for exploiting multi-component characteristics of ores in mineral processing circuits*. Dissertation, The University of Queensland.

GAO, P., ZHOU, W., HAN, Y., LI, Y., REN, W. 2020. *Enhancing the capacity of large-scale ball mill through process and equipment optimization: An industrial test verification,* Adv. Powder Tech., 31, 2079–2091.

GAULT, G.A. 1975. *Modelling and control of autogenous grinding circuit*. Dissertation, University of Queensland, Australia.

GUPTA, A., YAN, D. 2016. *Mineral processing design and operations*. Elsevier, 856.

HAHNE, R., PÅLSSON, B.I., SAMSKOG, P.O. 2003. *Ore characterisation for -and simulation of- primary autogenous grinding*. Min. Eng., 16, 13-19.

LATCHIREDDI, S.R. 2002. *Modelling the performance of grates and pulp lifters in autogenous and semi-autogenous mills*. Dissertation, University of Queensland, Australia.

LEUNG, K. 1987. *An energy based ore specific model for autogeneous and semi autogeneous grinding*, Dissertation, University of Queensland.

LYNCH, A.J. 1977. *Mineral crushing and grinding circuits, their simulation, optimisation, design and control*. Elsevier.

MORRELL, S., VALERY, W. 2001. *Influence of feed size on AG/SAG mill performance*. SAG Conference, Vancouver, BC, Canada.

MORRELL, S. 2004. *A new autogenous and semi-autogenous mill model for scale-up, design and optimization*. Min. Eng., 17, 437–445.

MUANPAOPONG, N., DAVÉ, R., BILGILI, E. 2022. *Impact of ball size distribution, compartment configuration, and classifying liner on cement particle size in a continuous ball mill.* Min. Eng., 189, 107912.

MUANPAOPONG, N., DAVÉ, R., BILGILI, E. 2023. *Application of TUSSIM with a variable Tromp curve for predicting optimal operation of multi-compartment mills with various ball size distributions.* Adv. Powder Tech., 34, 104171.

NAGESWARARAO, K. 1995. *A generalised model for hydrocyclones classifiers*. AusIMM Proceedings, 300, 2, 21 (Dec).

NAPIER-MUNN, T.J., MORRELL, S., MORRISON, R.D., KOJOVIC, T. 1996. *Mineral comminution circuits their operation and optimization*. JKMRC.

NARAYANAN, S.S., WHITEN, W.J. 1988. *Determination of comminution characteristics from single particle breakage tests and its application to ball mill scale-up*. Trans. Inst. Miner. Metall., 97, C115– C124.

STANLEY, G.G., 1974. *Mechanisms in the autogenous mill and their mathematical representation*. J. South Afr. Inst. Mining Metall., November, 77–98.

WHITEN, W.J., 1976. *Ball mill simulation using small calculators*. Proceedings AusIMM, 258, 47-53.